Title

Partitioning of Hexavalent Chromium in Temperature-Sensitive, Polyelectrolyte Hydrogels

Authors

Sassi, A.P.
Freed, D.
Blanch, H.W.
et al.

Publication Date

1994-12-01

LBL-36397
UC-401
Preprint

Lawrence Berkeley Laboratory
UNIVERSITY OF CALIFORNIA

CHEMICAL SCIENCES DIVISION

Submitted to Polymer Gels and Networks

Partitioning of Hexavalent Chromium in Temperature-Sensitive, Polyelectrolyte Hydrogels

A.P. Sassi, D. Freed, H.W. Blanch, and J.M. Prausnitz

December 1994

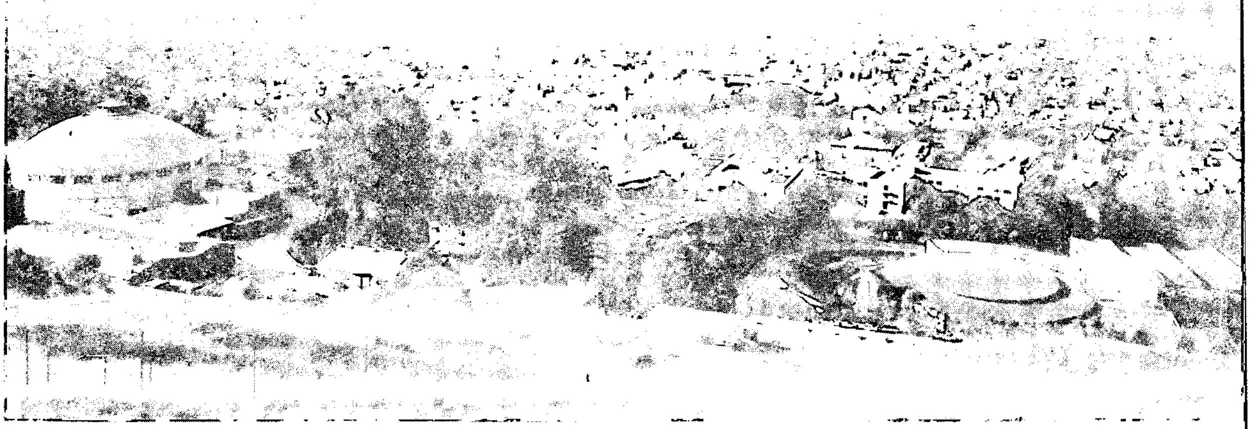

Prepared for the U.S. Department of Energy under Contract Number DE-AC03-76SF00098

DISCLAIMER

LBL-36397
UC-401

Partitioning of Hexavalent Chromium in Temperature-Sensitive, Polyelectrolyte Hydrogels

Alexander P. Sassi, David Freed, Harvey W. Blanch, and John M. Prausnitz*

Chemical Engineering Department
University of California

and

Chemical Sciences Division
Lawrence Berkeley Laboratory
University of California
Berkeley, California 94720

December 1994

*To whom correspondence should be addressed.

This work was supported by the Director, Office of Energy Research, Office of Basic Energy Sciences, Chemical Sciences Division, of the U.S. Department of Energy under Contract No. DE-AC03-76SF00098.

LBL-36397
UC-401

Partitioning of Hexavalent Chromium in Temperature-Sensitive, Polyelectrolyte Hydrogels

*Alexander P. Sassi, David Freed, Harvey W. Blanch and John M. Prausnitz**

Chemical Engineering Department
University of California, Berkeley
and
Chemical Sciences Division
Lawrence Berkeley Laboratory
1 Cyclotron Road
Berkeley, CA 94720

This work was supported by the Director, Office of Energy Research, Office of Basic Energy Sciences, Chemical Sciences Division of the U.S. Department of Energy under Contract Number DE-AC03-76SF00098.

*To whom correspondence should be addressed.

PARTITIONING OF HEXAVALENT CHROMIUM IN TEMPERATURE-SENSITIVE, POLYELECTROLYTE HYDROGELS

*Alexander P. Sassi, David Freed, Harvey W. Blanch and John M. Prausnitz**

Chemical Engineering Department, University of California, Berkeley

and

Chemical Sciences Division, Lawrence Berkeley Laboratory,

Berkeley, CA 94720

ABSTRACT

Partitioning data for hexavalent chromium (Cr(VI)) are presented for systems where thermally sensitive poly-N-isopropylacrylamide (NIPA)-based hydrogels are in contact with aqueous solutions of potassium dichromate ($K_2Cr_2O_7$). The poly-NIPA hydrogels contain 0-3% quaternized amine comonomer. Experimental results are given for the effect of gel charge, ionic strength, and temperature on the partitioning of Cr(VI) into these NIPA-copolymer gels. Swelling equilibria in aqueous $K_2Cr_2O_7$ solutions are compared to swelling in aqueous solutions of sodium chloride. Experimental partitioning data as a function of ionic strength and gel charge are compared with predictions based on several theoretical models for mixed electrolyte solutions. Predictions based on the cell model for polyelectrolyte solutions agree best with experimental results. Calculated results are in semi-quantitative agreement with experimental data for the effects of solution ionic strength and gel charge on Cr(VI) partitioning and in qualitative agreement for the effect of temperature.

*to whom correspondence should be addressed

I. INTRODUCTION

Hydrogels synthesized from N-isopropylacrylamide (NIPA) exhibit temperature-dependent swelling behavior. As temperature rises, at approximately 32-34°C, the volume of a poly-NIPA gel shrinks by an order of magnitude; various researchers have reported the swelling transition of a poly-NIPA gel to be continuous (1-4) or discontinuous (5, 6). The dramatic shrinking of poly-NIPA hydrogels is related to the lower consolute solution temperature (LCST) behavior of aqueous solutions of uncrosslinked poly-NIPA (7); upon decreasing the temperature below the LCST, the uncrosslinked poly-NIPA solution moves from the two-phase region to the single-phase region because hydrogen-bonding interactions between the polymer and water dominate polymer-water phase behavior.

Because the water content of poly-NIPA gels can be controlled by solution temperature at near-ambient conditions, poly-NIPA gels have sparked interest for novel applications in drug delivery and solute recovery. Applications for drug delivery have been studied by Hoffman and co-workers (8) and Okano et al (9). For solute recovery, two processes have been proposed; these are illustrated in Figures 1a and 1b. In one process, (Figure 1a) proposed by the authors (10), a solute (or solutes) partitions into the highly-swollen hydrogel at temperatures below the transition temperature. The gel containing the solute(s) of interest is then removed and collapsed at a temperature above the transition temperature, releasing the imbibed solutes. The gel can then be recycled by cooling it to the lower temperature. In the other process (Figure 1b), proposed originally by Cussler et al (11), a size-dependent separation is obtained by placing the deswollen hydrogel in contact with the feed solution at low temperature to absorb water and low-molecular solutes, which are then recovered by collapsing the gel at a higher temperature. In this second process, the desired, high-molecular-weight solute is concentrated in the raffinate solution. Cussler's process has been studied in applications of coal de-watering (12, 13), soy-protein concentration (4), viral concentration (5), and enzyme concentration (14).

By copolymerizing NIPA with other monomers, the magnitude and temperature range of the swelling transition can be adjusted, providing extra control of the water content for applications. For example, copolymerization with a more hydrophobic monomer, such as N-tert-butyl acrylamide, decreases the transition temperature as well as the water content of the gel (1). Copolymerization with a more hydrophilic monomer, such as an ionized monomer, increases swelling, transition temperature and the temperature range where the collapse occurs. In addition, the swelling properties of the polyelectrolyte gel depend on ionic strength. Temperature-dependent swelling equilibria of copolymer gels of NIPA and a strong electrolyte, [(methacrylamido)propyl] trimethylammonium chloride (MAPTAC), have been measured in solutions of differing ionic strength (2). MAPTAC, a quaternized amine, has a positive charge.

Distribution coefficients for a solute between the hydrogel and its surrounding solution are essential for design of applications for novel thermo-sensitive hydrogels, as well as for established applications of gels as, for example, contact lenses, biomaterials, chromatographic resins, and electrophoresis media. The equilibrium distribution of a macromolecular solute, such as a protein, between a solution and a gel depends on the delicate balance of steric exclusion and electrostatic and short-range intermolecular forces. Here we report studies of the partitioning of a salt into a polyelectrolyte gel to better understand the effects of electrostatics in a system less complex than that containing proteins. Our hydrogel is a copolymer of NIPA and MAPTAC, corresponding to earlier studies of swelling equilibria (2). We use potassium dichromate ($K_2Cr_2O_7$) for the salt as an example of a multicomponent electrolyte solution which contains several ionic species. Chromates (unlike many buffer salts) can be assayed easily by measuring absorption of visible light. Removal of trace amounts of hexavalent chromium (less than 25 mg/L Cr(VI)) from wastewater and cooling-tower blowdown by ternary and quaternary amine-functionalized anion-exchange resins is also of practical concern (15-20).

II. EXPERIMENTAL

Materials

N-isopropylacrylamide (NIPA), N,N'-methylene bisacrylamide (BIS), electrophoresis grade, and ammonium persulfate (APS) were purchased from Eastman Kodak. [(Methacrylamido)propyl]trimethylammonium chloride (MAPTAC) was purchased as a 50% solution in water from Monomer-Polymer and Dajac Laboratories. Sodium metabisulfite (SMB) was purchased from Sigma. Potassium dichromate was purchased from Fisher. All reagents were used as received. Distilled water was filtered (0.2 μm) and deionized (17.9 MΩ-cm resistivity) with a Barnstead Nanopure II unit.

Hydrogel Synthesis

Uncharged hydrogels were synthesized by free-radical, solution copolymerization of NIPA and BIS, the crosslinking agent. Cationic hydrogels were synthesized by copolymerization of NIPA, BIS and MAPTAC. The redox couple APS/SMB was used to initiate polymerization.

All gels were prepared in aqueous solution according to methods in reference (2). For each gel, the desired amounts of NIPA and BIS were dissolved in 96 mL water. Separate solutions of APS and SMB were also prepared (0.1 g/20 mL each). The solutions were degassed under a 27-inch Hg vacuum for 90 minutes and subsequently transferred to a nitrogen-containing glove box. The appropriate volume of 50% MAPTAC solution was added to the monomer solution, and 2 mL SMB solution and 2 mL APS solution were added. The resulting solution was stirred with a magnetic stir bar for one minute and then injected quickly into molds chilled in the freezing compartment of a standard refrigerator. The molds were made of two glass plates (10 x 10 cm) separated by 1.57 mm Teflon spacers and held together using Teflon tape, duct tape, and binder clips. The molds were then placed in a refrigerator at 10° C so that the reaction temperature would not exceed the phase-transition temperature of the forming polymer. After 48 hours, disks one centimeter in diameter were cut from the resulting gel slabs using a punch. The gels were soaked in water for one week at 10°C, changing water daily to leach out any unreacted monomer.

Three variables were used to characterize the nominal composition:

%T = mass of all monomers (g)/volume of water (mL) x 100
%C = moles of cross-linking monomer/total moles of monomer x 100
%CM = moles of co-monomer in feed/total moles of monomer x 100

The gels synthesized were 15 %T and 1 %C; these parameters were chosen so that gels would be highly swollen yet durable enough not to break apart from the handling and agitation during the partitioning experiment. Gels were made at 0, 1, 2, and 3 %CM (= %MAPTAC) to produce a series of gels with varying charge density.

Swelling Measurements

To determine the degree of swelling in salt solutions, gels were taken from water at 10° C, weighed, and placed in salt solution. The gels were blotted carefully with a Kim-Wipe to remove surface water before weighing; this technique was found to be reproducible to within 1-2%. The solutions were incubated in a Blue M Electric Company Shaker Bath, Model MSB-3222A-1. The gels were weighed daily until swelling equilibrium was established; in approximately one week for most solution conditions. Each time the gels were weighed, the salt solution in each beaker was replaced with fresh solution of the same ionic strength. This procedure gave the swelling ratio at equilibrium in salt solution relative to that in water at 10 °C. Additionally, gels were taken from water at 10 °C, weighed, and dried to constant weight on aluminum foil at ambient temperatures in a fume hood. This procedure gave the swelling ratio at equilibrium in water at 10°C relative to the "dry" weight. Gels were also dried in a warm oven under a 27-inch Hg vacuum; however, in some cases the gels burst during this process. Because the swelling ratio was found not to depend on the method of drying, the gels were dried instead at ambient temperatures.

Partitioning Measurements

Gels were taken from water at 10 °C, weighed, and placed in a beaker with a known mass of aqueous potassium dichromate of known concentration. The beakers were incubated with gentle shaking in the shaker bath at the desired temperature. After equilibrium was reached, the gels were removed from the beakers and weighed again. The absorbance of the remaining solution in each beaker was measured at 346 nm with a Shimadzu UV-160 Spectrophotometer using distilled, deionized water as the reference. The concentration of hexavalent chromium (Cr(VI)) was determined from the relationship of the absorbance at 346 nm to potassium dichromate concentration of standard solutions, as discussed below. Where necessary, appropriate dilutions were carried out to assure that Beer's law was valid.

When potassium dichromate dissolves in solution, several Cr(VI)-containing chromate ions are formed. The following two ionic equilibria are most important (17, 21):

$$HCrO_4^- \leftrightarrow H^+ + CrO_4^{2-}\,,\ pK = -6.5$$
$$2HCrO_4^- \leftrightarrow Cr_2O_7^{2-} + H_2O\,,\ pK = 1.52$$

In dilute solutions (chromium concentrations less than about 100 mg/L) between pH 2.0-6.5, the bichromate ion, $HCrO_4^-$, is the prevailing species. After dilution, the chromium concentrations and pH fell well within this range for all samples analyzed by spectrophotometry. Equilibrium calculations using the pK values given above demonstrated that approximately 96% of the chromium was present as $HCrO_4^-$. The wavelength used, 346 nm, is about 5 nm less than the wavelength where $HCrO_4^-$ and CrO_4^{2-} ions have the same molar absorbance (the isobestic point)(22); the presence of CrO_4^{2-} did not significantly affect the applicability of Beer's law. The trace concentration of $Cr_2O_7^{2-}$ did not affect the applicability of Beer's law either. Because the concentrations used for the calculation of the partition coefficient were based on analysis for $HCrO_4^-$ as the sole chromium-containing species, the partition coefficient reflects the distribution of hexavalent chromium, rather than that of a specific chromate.

Knowing the initial and final gel masses, the initial solution mass, and the initial and final solution concentrations, it was possible to calculate the concentration of chromate in the gel at equilibrium. The equilibrium distribution of solute between the gel and solution phases was defined by the partition coefficient, K:

$$K = \frac{\text{moles of Cr(VI)/ g swollen gel}}{\text{moles of Cr(VI)/ g solution}}$$

III. EXPERIMENTAL RESULTS

Swelling Equilibria in $K_2Cr_2O_7$ Solutions

Figure 2 presents swelling equilibria at 10°C in water (ionic strength 10^{-7} mol/kg), potassium dichromate solutions (symbols) and sodium chloride (NaCl) solutions (dashed lines) for poly-NIPA/MAPTAC gels of 0-3% CM. Experimental data for swelling equilibria in potassium dichromate solutions are also presented in Table 1. Swelling equilibria in NaCl solutions were taken from reference (2). In general, at low ionic strength and in water, swelling increases with gel charge (%CM). As ionic strength increases, the charged gels shrink, while the uncharged gel (0%CM) does not. The dependence of swelling on salt concentration is usually modelled by Donnan-type equilibria; such models predict that K tends towards unity as ionic strength of the surrounding solution increases. In turn, a more equal distribution of ionic species (partition coefficients closer to unity) results in a lower "swelling pressure," or driving force for swelling. Hence, the collapse of polyelectrolyte gels in salt solutions is expected.

In aqueous potassium dichromate solutions, polyelectrolyte gels swell less than in sodium chloride solutions of the same ionic strength. Because fewer divalent ions are necessary to satisfy electroneutrality in the gel, the osmotic swelling pressure is lower for a solution containing divalent ions at any given ionic strength, and hence the swelling in such a solution is also lower . Although the ratio of divalent anions to univalent anions never exceeds 15% for the potassium dichromate solutions used here, the concentration of divalent ions was found to be higher in the gel phase of anion exchange resins used for Cr(VI) removal (15, 16). Similar effects of salt chemistry on gel swelling have been reported earlier (23, 24)

Partitioning of Cr(VI) Anions

Figure 3 presents experimental data for the partition coefficients of Cr(VI) into NIPA/MAPTAC gels of 0-3% CM in aqueous potassium dichromate solutions at 22°C. Data also appear in Table 2. The partition coefficient, K, is plotted against the ionic strength (mol/kg) of the initial (feed) solution. At each ionic strength, the partition coefficient increases with % MAPTAC, as expected because Cr(VI) ions are negatively charged, whereas MAPTAC is positively charged. For a given gel chemistry, partitioning of an ion into an oppositely-charged gel is lower at higher ionic strength, as predicted by simple Donnan equilibria arguments. In potassium dichromate solutions of high ionic strength, a smaller fraction of the total Cr(VI) in the system is associated with the charges in the gel than in low-ionic-strength solutions because the number of charges on the polymer chains is fixed by the % MAPTAC. Therefore, the partition coefficient decreases as the ionic strength increases.

Figure 4 presents experimental data for the partition coefficients of Cr(VI) into NIPA/MAPTAC gels of 0-3% CM at three temperatures. Data are reported in Table 3. The initial molality of Cr(VI) was 0.0005 mol/kg (26 mg/L) for all cases. In the uncharged gel, the partition coefficient decreases when the temperature rises from 25 to 33.4°C. In the absence of favorable interactions between the salt and polymer, the partition coefficient for a salt in an uncharged gel should exhibit the same trend with temperature as that for swelling. The swelling ratio at 33°C for poly-NIPA is slightly lower (8%) than that at 25°C; therefore, one might expect K to fall. For each of the charged gels, K increases slightly between 25 and 33.4° C and then more dramatically between 33.4°C and 40°C, depending on the extent of gel collapse. As shown by Beltrán et al, the collapse transition for NIPA/MAPTAC gels moves to higher temperatures and becomes more gradual as %MAPTAC increases (2). At 40°C, the 1 %MAPTAC gel has collapsed much more (relative to its mass at 33°C) than the 3 %MAPTAC gel; therefore, the resulting concentration of MAPTAC (and hence fixed-charge density) does not rise with %MAPTAC at 40°C. K for Cr(VI) should increase with charge density, just as at ambient temperatures, as observed. One might expect then, that at temperatures well above the collapse transition for the 3% gels, K would be again highest for the 3%MAPTAC gel, as observed (data not shown here).

Figure 5 presents the same data as those in the previous figure but in terms of loading on a dry-polymer basis (mol Cr(VI)/g dehydrated gel) as a function of %CM. By examining the loading of Cr(VI), we eliminate the confounding effect of swelling on comparison of data at different %CM. Loading increases with the amount of charge on the gel network at all temperatures, as expected. Between 25 and 33.4°C, there is little difference in the loading; therefore, differences in K are due primarily to differences in swelling. Loading declines at 40°C, suggesting that Cr(VI) is less favored in the more hydrophobic, partially collapsed gel.

IV. COMPARISON OF MODEL WITH THEORY

For a small solute in a highly swollen gel, steric hindrance should be negligible. In the limit that the solute size approaches the size of a water molecule, the partition coefficient for a solute should equal the fractional water content of the hydrogel, provided that the network is inert to the solute. Given that the effect of steric hindrance is taken into account through the swelling, and assuming that the gel is so highly swollen that the polymer has little effect on the solvent activity coefficient in the gel phase, a molecular-thermodynamic description of a multicomponent solution can be used to predict the distribution of a solute between the external solution and the water inside the gel. Some authors assume the solute has no interaction with the polymer other than that of excluded volume and calculate the partition coefficient as the ratio of the solute concentration with respect to the volume of water in the gel phase (rather than the total volume of the gel phase) and the solute concentration in the surrounding solution. In this case, the product of the distribution coefficient obtained from the thermodynamic description and the hydration (fractional water content of the gel) should equal the experimentally determined partition coefficient :

$$K_{exp} = HK_{model} \tag{1}$$

where K_{exp} is the experimental partition coefficient, H is the fractional water content of the gel (hydration), and K_{model} is the solute distribution predicted by a molecular-thermodynamic model for multicomponent solutions wherein the polymer has not been included as a volume-occupying component.

There are two types of theories for the electrostatic energy of a system, both based on the Poisson-Boltzmann equation of electrostatics, which we may apply to calculate thermodynamic properties of the gel phase when the gel itself is charged. We can use a model where the gel phase is described in terms of a solution of charged, hard spheres (including the polymer charges, counterions and added ions), or we can use a model where the gel phase is described in terms of charged, hard spheres (the counterions to the polymer and the added ions) and cylinders (the polymer backbone).

Examples of the former type of model are the Debye-Hückel (25), the Mean Spherical Approach (26, 27) and Pitzer's model for electrolyte solutions (28, 29), which are based on solving the Poisson-Boltzmann equation for the mean charge density as a function of radial distance from a mobile, spherical ion in a solution of other mobile, spherical ions. The Debye-Hückel, Mean Spherical Approximation and Pitzer's expressions for ionic activity coefficients are given in Appendix C. Pitzer's expressions include short-range ion-ion attractive forces in addition to electrostatics.

An example of the latter type is the cell model for polyelectrolyte solutions used by Katchalsky, which is based on solving the Poisson-Boltzmann equation for the electrostatic potential as a function of radial distance from the axis of a charged hard cylinder in a solution ("a cell") of spherical ions (31-33). The ionic activity coefficients in the cell model used here, taken from the work of Guerón and Weisbuch, are given in Appendix D (34).

In both types of models, the charges on the polymer are not included in the parameter which characterizes the mean electrostatic screening due to the presence of multiple ions in the solution. Hence, in the hard-sphere-only models, the charge on the polymer backbone enters in the calculations only through the requirement that the gel phase must be electrically neutral. In the cell-type model, the electrostatic potential to which the ions respond is a result of polymer-ion interactions, while in the hard-sphere model, the electrostatic potential to which the ions respond is a result only of ion-ion interactions. Both theories imply certain geometrical assumptions about the gel phase which are not correct. For example, the charges on the polymer are neither freely-mobile, charged, hard spheres (as in the standard Debye-Hückel treatment) nor are they located on a rigid cylinder (as in the Cell Model); we expect that the polymer strands adopt a conformation constrained due to crosslinks and entanglements but not so much so as to be rigid. Therefore, neither model will correctly account for the entropy of the charged groups. We wish to determine which type of model gives the best agreement between experimental and calculated partition coefficients for ions partitioning into polyelectrolyte, temperature-sensitive hydrogels of low charge density.

To evaluate K_{model}, the theoretical distribution coefficient, we begin with the principle that at equilibrium, the chemical potential of a mobile, neutral component must be the same in every phase:

$$\mu_i' = \mu_i'' \tag{2}$$

where μ_i is the chemical potential of component i, and where ' and " denote the bulk solution and the solution in the gel phase, respectively. For a solute component i in a solvent o, the chemical potential, μ_i, can be derived from the Helmholtz energy, A:

$$\mu_i = \left(\frac{\partial A}{\partial n_i} \right)_{T,V,n_j,j \neq i} \tag{3}$$

where n is the mole number.

In the calculation of phase equilibria, one often uses the concept of activity, a, which, in part, expresses deviations from a reference (standard) state through the activity coefficient. The chemical potential can then be written as the following:

$$\mu_i = \mu_i^o + RT \ln a_i = \mu_i^o + RT \ln \frac{\gamma_i m_i}{m_i^o} \tag{4}$$

where μ_i^o is the chemical potential of component i in the standard state, m_i is a measure of the concentration of component i (here taken to be the molality), m_i^o is the respective concentration in the standard state, and γ_i is the activity coefficient of component i, with respect to the chosen standard state. The standard state is a hypothetical, ideal, dilute solution at system temperature, pressure and at fixed concentration m_i^o usually set to unity. In an ideal, dilute solution, γ_i always equals one.

The activity coefficient γ_i is related to the partial derivative of the excess Helmholtz energy:

$$RT \ln \gamma_i = \left(\frac{\partial A^{ex}}{\partial n_i} \right)_{T,V,n_j,j \neq i} \tag{5a}$$

where the excess Helmholtz energy is given by the difference of the total Helmholtz energy and that of a reference solution:

$$A^{ex} = A - A^{ideal} \tag{5b}$$

The excess Helmholtz energy due to coulombic interactions (the electrostatic Helmholtz energy) as used herein is in reference to a solution of identical composition but where all the molecules are uncharged. The electrostatic Helmholtz energy can be obtained by integrating with respect to charge the electrostatic potential obtained from the solution of the Poisson-Boltzmann equation (25).

In expressions for the electrostatic Helmholtz energy of an electrolyte solution amenable to phase-equilibrium calculations, the solvent is not considered as a component but is instead characterized as a dielectric continuum. Expressions of this type are said to be developed in the McMillan-Mayer framework. Experimental results are obtained under conditions corresponding to the Lewis-Randall framework. Fortunately, one is able to convert chemical potentials from those calculated in the McMillan-Mayer framework to those in the Lewis-Randall framework. Among others, Haynes et al have discussed the application of this conversion between frameworks (35). Haynes noted improved agreement between experimental data for activity coefficients of electrolytes and calculated activity coefficients where these were converted from the McMillan-Mayer framework to the Lewis-Randall framework (35). The chemical potential in the Lewis-Randall framwork can be obtained from that in the McMillan-Mayer framework by adding the term $-P^{ex}\overline{V}_i$

$$\mu_i = \mu_i^o + RT\ln\frac{\gamma_i m_i}{m_i^o} - P^{ex}\overline{V}_i \tag{6}$$

where $\overline{V}_i$ is the partial molar volume of the component i, and P^{ex} is the excess pressure, obtained from the partial derivative of A^{ex} with respect to volume.

We must also account for the increased osmotic pressure (relative to the external solution, or bath, phase) encountered by a solute in the gel phase. The hydrostatic pressure of the bath is different from that in the gel because the composition of the two phases can never be identical, as the polymer is constrained by chemical crosslinks and physical entanglements. At equilibrium, the pressure due to network elasticity must balance the osmotic pressure of the gel phase. The chemical potential in the gel phase is then the following:

$$\mu_i'' = \mu_i^{o''} + RT\ln\frac{\gamma_i'' m_i''}{m_i^{o''}} - P^{ex''}\overline{V_i} + \Delta\Pi_{elastic}\overline{V_i} \tag{7}$$

where $\Delta\Pi_{elastic}$ is the elastic contribution to the swelling pressure of the gel. Here, $\Delta\Pi_{elastic}$ is evaluated using a model for the elastic Helmholtz energy of a swollen gel, such as the affine or phantom models (36, 37). The correction to the chemical potential arising from $\Delta\Pi_{elastic}$ is negligible for our systems because the partial molar volumes of the ions are small.

If we take the standard state to be the same for both phases, we calculate the partitioning of a component i by determining the concentrations (molalities) of component i in each phase which satisfy the following equation (obtained from equations 2, 6 and 7):

$$\gamma_i' m_i' = \gamma_i'' m_i'' \exp\left(\frac{\overline{V_i}\left(\Delta\Pi_{elastic} + P^{ex'} - P^{ex''}\right)}{RT}\right) \tag{8}$$

If component i is a salt, the experimental activity coefficient is often reported as mean ionic activity coefficient, $\gamma_\pm$. The mean ionic activity coefficient for a salt is related to the activity coefficients of the individual cations and anions:

$$\gamma_\pm^{(\nu_+ + \nu_-)} = (\gamma_+)^{\nu_+}(\gamma_-)^{\nu_-} \tag{9}$$

where ν is the stoichiometric coefficient of the ion in the neutral salt, and subscripts + and - denote cation and anion, respectively. Single-ion activity coefficients can be obtained from theory.

Chemical equilibrium constants relating the concentrations of the different Cr(VI) anions are known, and the number of charges on the polymer network is fixed; we use the nominal %CM and the experimental swelling ratio to calculate the charge density of the gel phase. Therefore, the composition of each phase can be specified by two independent components, one neutral salt (such as $K_2Cr_2O_7$ or $KHCrO_4$) and water, which provides a source of H^+ ions.

To solve for the distribution of Cr(VI) between the phases, we used two algorithms. In the first algorithm (here called the rigorous algorithm), we determined the concentrations of each of the six ions ($Cr_2O_7^{2-}$, $HCrO_4^-$, CrO_4^{2-}, K^+, H^+, OH^-) in the bath using the equilibrium relationships between the chromate anions. We then applied equation 2 to the salt $K_2Cr_2O_7$ and solved for the concentration of each ion of the salt ($Cr_2O_7^{2-}$, K^+) in the gel. The equilibrium relationships between the chromate anions were again used to determine the concentrations of the other ions in the gel. Once the composition of each phase is known, K_{model} can be calculated. We discuss the rigorous algorithm in Appendix A. In the calculations, we assume that the pH is the same in both phases. The activities of hydrogen ion and hydroxide ion are virtually the same in both phases because the $\Delta\Pi_{elastic}$-related correction to the activity is negligible. We also constrain each phase to be electrically neutral.

We also investigated a second algorithm (here called the pseudo-one-component algorithm) to estimate the partition coefficient; this algorithm ignores the explicit presence of multivalent ions. The pseudo-one-component algorithm is computationally much simpler and results in calculated partition coefficients which agree better with our experimental data over a larger range of conditions. In the pseudo-one-component algorithm, we first calculate the ionic strength of the bath solution containing the six ions and then use equation 2 to calculate the partitioning of a strong 1-1 salt (NaCl) where the concentration of the 1-1 salt in the hypothetical bath solution is the same as the ionic strength of the experimental bath solution. The calculated partition coefficient of Cr(VI) (K_{model}) is taken to be the calculated partition coefficient of the monovalent anion. We discuss the pseudo-one-component algorithm in Appendix B.

Figure 6 compares experimental and calculated partition coefficients for Cr(VI) in 0-3% CM NIPA/MAPTAC gels where the initial molality of $K_2Cr_2O_7$ was 0.0025 mol/kg. Data are reported in Table 4. Figure 6 shows the results obtained by using different activity-coefficient models and algorithms to calculate the activity coefficients. The calculated results obtained using the pseudo-one-component algorithm lie closest to the experimental data. Using the rigorous algorithm and assuming all activity coefficients to be unity results in the poorest agreement with experimental data. Agreement between calculated and experimental partition coefficients improves significantly when a model such as Pitzer's is used to calculate ionic activity coefficients for the rigorous algorithm. Calculated results were insensitive to the activity-coefficient model; they were nearly the same for the Debye-Hückel, Mean Spherical Approximation or Pitzer's model. Figure 6 shows only results using Pitzer's model. Activity-coefficient expressions developed by Guerón, who used the cell-model approach, give the best agreement with experimental data.

The partition coefficients calculated using the pseudo-one-component algorithm with activity coefficients of unity, or those calculated with Pitzer's model, are virtually the same as the partition coefficients calculated for Cr(VI) using the rigorous algorithm with Guerón's expression for activity coefficients. Using Guerón's expressions to evaluate activity coefficients in the pseudo-one-component algorithm gives only slightly better agreement with experimental data. In all our calculations, the charge on the polymer backbone was determined by using the nominal %CM; if the actual %CM were lower than the nominal value (due to incomplete incorporation of the comonomer into the gel), agreement between calculation and experiment would improve. Although agreement is not quantitative, we obtain much better estimates of Cr(VI) partitioning if we use the cell model to calculate partitioning of a univalent anion in a 1-1 system than any algorithm that considers the three chromate anions and one cation. It is much easier to solve for the distribution of a monovalent salt as opposed to a multivalent salt.

Figure 7 presents a comparison of calculated and experimental partition coefficients for Cr(VI) in 1-3%CM NIPA/MAPTAC gels as a function of ionic strength. Data are reported in Table 1. The calculated partition coefficients were obtained using the cell-model and the pseudo-one component algorithm. The calculated partition coefficients show fair agreement with experimental data except at the lowest ionic strength. At this low ionic strength, inclusion of activity coefficients has a negligible effect on the calculated partition coefficients, as expected. The external ionic strength is approximately ten or more times lower than the charge density of the polymer in the gel phase. Thus, the experimental data may be significantly affected by the relative affinity of the amine of MAPTAC towards different counterions, because the chromate anions are significantly diluted by the original counterions of the polymer charges contained by the gel. Because we did not assay for the original counterions of the polymer charges, we cannot account for them quantitatively for the purposes of model calculations, but we know that the calculated partition coefficients would be lower if the original counterions were taken into account.

Figure 8 presents calculated partition coefficients of Cr(VI) into NIPA/MAPTAC gels of 0-3% CM at three temperatures, corresponding to the experimental data shown in Figure 4. Data are reported in Table 2. The partition coefficients in Figure 8 were obtained as for the preceding figure. Calculated results are not in quantitative agreement with experiment because the ionic strength of the bath is smaller than the concentration of charges on the polymer backbone. However, we obtain the correct qualitative trends in partition coefficient with temperature for the polyelectrolyte gels; the partition coefficient increases dramatically upon collapse of the gel with temperature.

V. CONCLUSIONS

Swelling of poly-NIPA/MAPTAC hydrogels in aqueous potassium dichromate solutions is similar to that in aqueous sodium chloride solutions. At low ionic strengths, swelling is a strong function of %CM (gel charge); greater swelling is obtained for gels with more MAPTAC. At higher, but still moderate ionic strengths (0.1 mol/kg), the gel charge has a markedly lower effect on gel swelling. Swelling in aqueous potassium dichromate is lower than that in sodium chloride solutions for ionic strengths up to approximately 0.01 mol/kg, possibly because of the presence of divalent chromate ions $Cr_2O_7^{2-}$ and CrO_4^{2-}.

At low ionic strengths, the partition coefficient K for Cr(VI) is highly dependent on gel charge. This dependence is diminished with increasing ionic strength. At 0.1mol/kg $K_2Cr_2O_7$ in the feed solution, the partition coefficients for the gels differ only slightly and are virtually unity. The effect of rising temperature is to increase K, mainly due to highly reduced swelling as the gel undergoes its temperature-dependent collapse.

Fair agreement is obtained between experimental and predicted partition coefficients for the effects of gel charge and ionic strength using the pseudo-one-component algorithm with ionic activity coefficients calculated using the cell-model-based-approach of Guerón and Weisbuch (34). While all theoretical methods used to calculate partitioning predicted the correct qualitative trends of partition coefficient with temperature and ionic strength, the Cr(VI) partition coefficient was best predicted by the pseudo-one-component algorithm. Calculations with the pseudo-one-component algorithm are much simpler than those using more rigorous methods. For development of a reliable quantitative theory, likely requirements are independent data on possible ion-polymer non-electrostatic interactions and more extensive characterization of the polymer network.

ACKNOWLEDGMENTS

This work was supported by the Director, Office of Energy Research, Office of Basic Energy Sciences, Chemical Sciences Division of the U.S. Department of Energy under Contract No. DE-AC03-76SF00098 and by the National Institutes of Health. The authors are grateful to John Baker, Sagrario Beltrán, John Newman, Kenneth Pitzer, and Clayton Radke for many helpful comments. APS is grateful to the National Science Foundation for a fellowship.

FIGURE CAPTIONS

Figure 1a. Method proposed by Prausnitz and Blanch for using gels as concentrating agents.

Figure 1b. Method proposed by Cussler and co-workers to use gels as concentrating agents.

Figure 2. Swelling equilibria at 10 °C for poly-NIPA/MAPTAC copolymer gels in water and in aqueous solutions of potassium dichromate or sodium chloride. Results at 10^{-7} mol/kg represent swelling in deionized water. Lines are drawn to guide the eye. Bold lines denote swelling in potassium dichromate solutions, and dashed lines denote swelling in sodium chloride solutions.

Figure 3. Experimental partition coefficients at 22 °C for Cr(VI) in poly-NIPA/MAPTAC copolymer gels as a function of initial solution ionic strength. Lines are drawn to guide the eye.

Figure 4. Experimental partition coefficients for Cr(VI) in poly-NIPA/MAPTAC copolymer gels as a function of temperature for initial Cr(IV) molality of 0.00025 mol potassium dichromate/kg. Lines are drawn to guide the eye.

Figure 5. Experimental loading of Cr(VI) into poly-NIPA/MAPTAC gels at 25, 33.4 and 40 °C as a function of gel charge (%CM). Lines are drawn to guide the eye.

Figure 6. Experimental (points) and calculated (lines) partition coefficients for Cr(VI) partitioning into 0-3%CM poly-NIPA/MAPTAC gels from a solution of initial molality of 0.0025 mol potassium dichromate/kg at 22°C. The lines denote different calculations. The uppermost, solid line represents calculations using the cell-model-based activity coefficient expressions of Gueròn and Weisbuch and the pseudo-one-component algorithm (34). The

lowermost, dashed line represents calculations using the rigorous algorithm, accounting for all the chromate anions, and assuming that all activity coefficients are equal to unity.

Figure 7. Experimental (closed symbols) and calculated (open symbols) partition coefficients for Cr(VI) in poly-NIPA/MAPTAC gels at 22°C in aqueous solutions of potassium dichromate as a function of initial solution molality. Lines are drawn to guide the eye. Calculations were performed using the activity coefficient expressions of Guerón and Weisbuch in the pseudo-one-component algorithm for the poly-NIPA/MAPTAC gels (34).

Figure 8. Calculated partition coefficients for Cr(VI) as a function of temperature in 1-3% poly-NIPA/MAPTAC gels, corresponding to the experimental conditions in Figure 4. Calculations were performed using the expressions of Guerón and Weisbuch in the pseudo-one-component algorithm.

Figure 1a

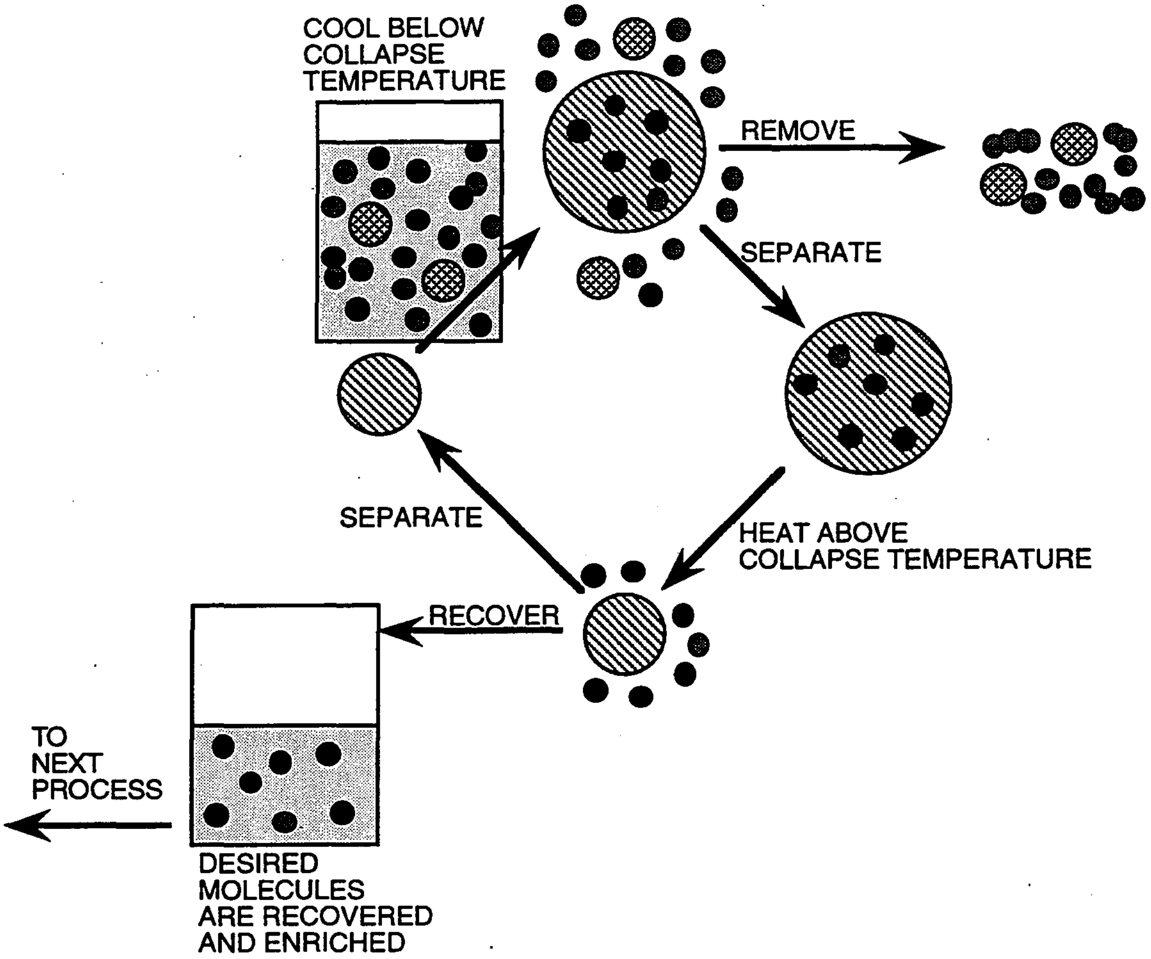
COOL BELOW
COLLAPSE
TEMPERATURE
REMOVE
SEPARATE
HEAT ABOVE
COLLAPSE TEMPERATURE
SEPARATE
RECOVER
TO
NEXT
PROCESS
DESIRED
MOLECULES
ARE RECOVERED
AND ENRICHED

Figure 1b

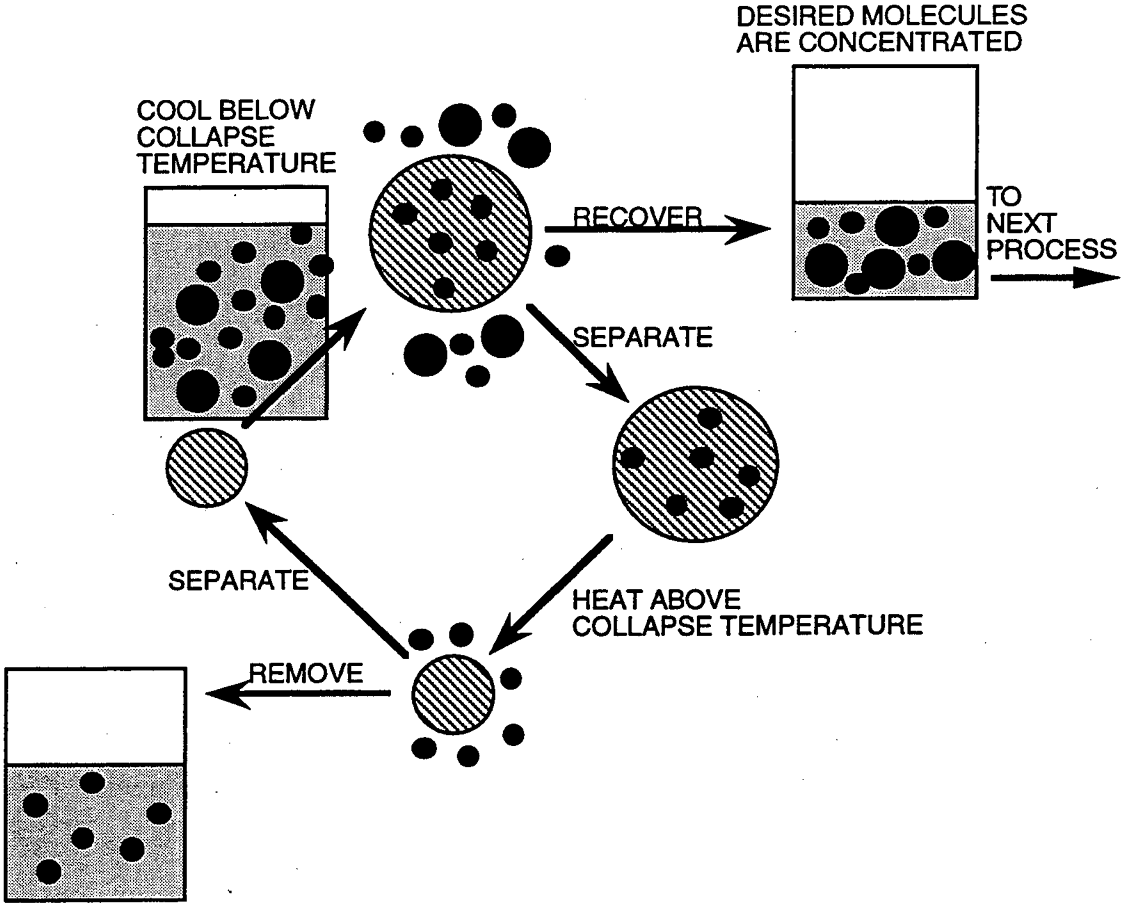
DESIRED MOLECULES ARE CONCENTRATED
COOL BELOW COLLAPSE TEMPERATURE
RECOVER
TO NEXT PROCESS
SEPARATE
HEAT ABOVE COLLAPSE TEMPERATURE
SEPARATE
REMOVE

Figure 2

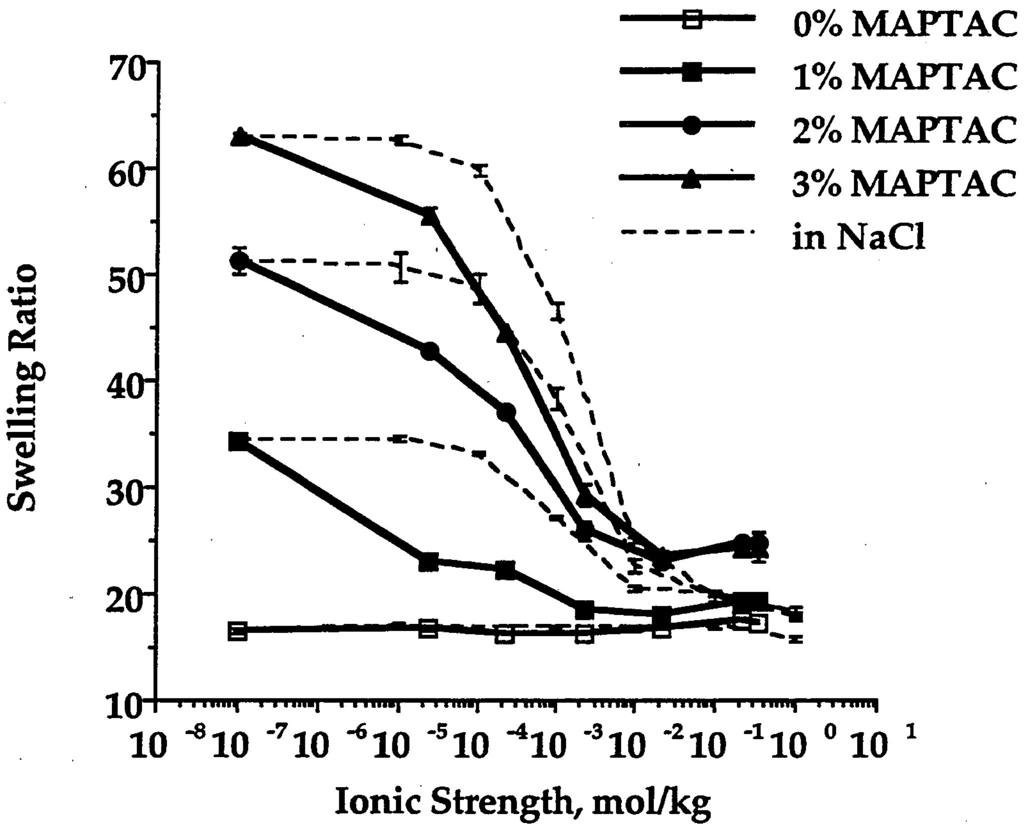
0% MAPTAC
1% MAPTAC
2% MAPTAC
3% MAPTAC
in NaCl
Swelling Ratio
70
60
50
40
30
20
10
10 -8
10 -7
10 -6
10 -5
10 -4
10 -3
10 -2
10 -1
10 0
10 1
Ionic Strength, mol/kg

Figure 3

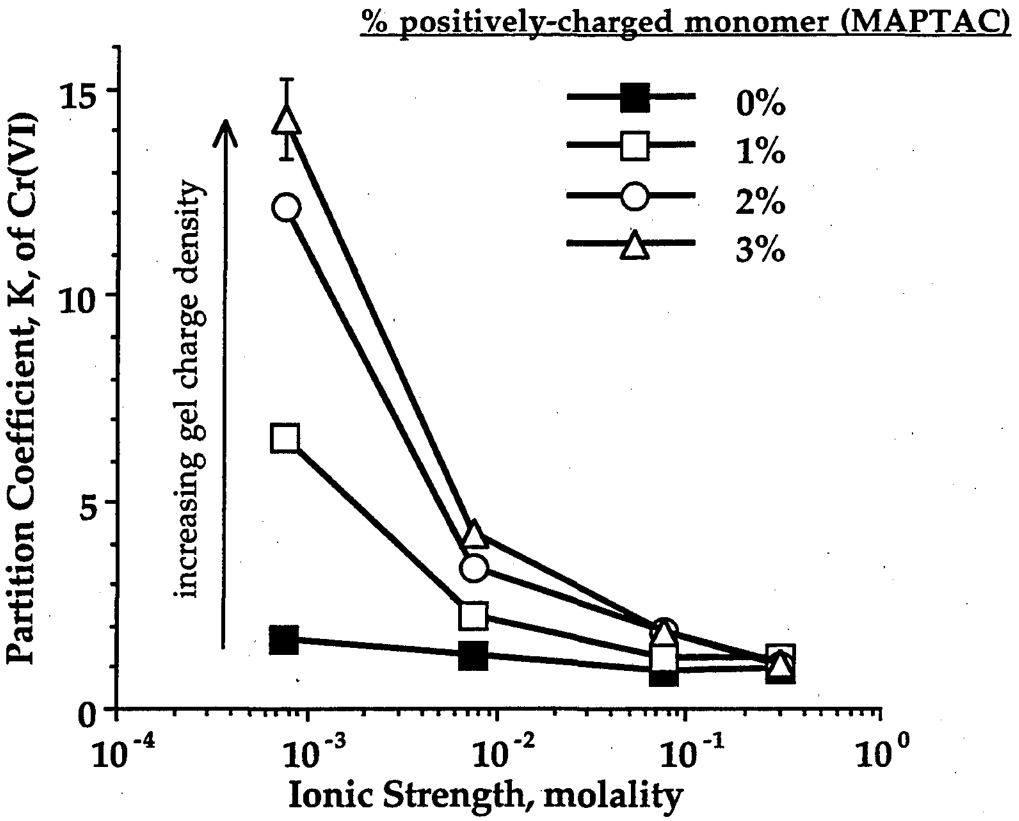
% positively-charged monomer (MAPTAC)
0%
1%
2%
3%
increasing gel charge density
Partition Coefficient, K, of Cr(VI)
0
5
10
15
10^-4
10^-3
10^-2
10^-1
10^0
Ionic Strength, molality

Figure 4

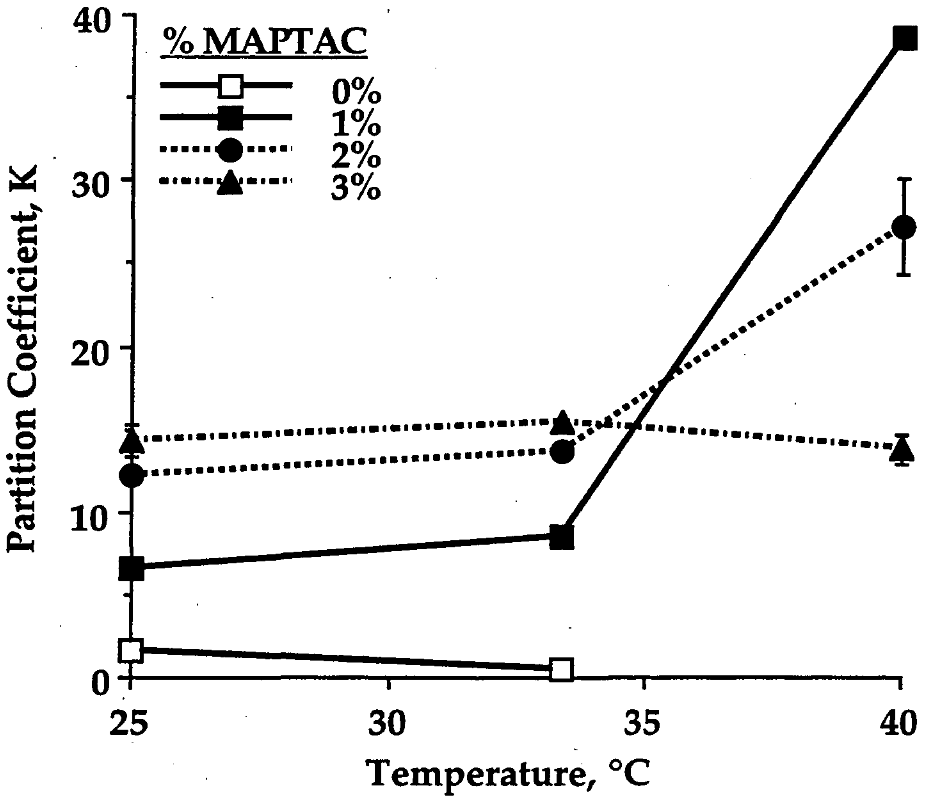
% MAPTAC
0%
1%
2%
3%
Partition Coefficient, K
0
10
20
30
40
25
30
35
40
Temperature, °C

Figure 5

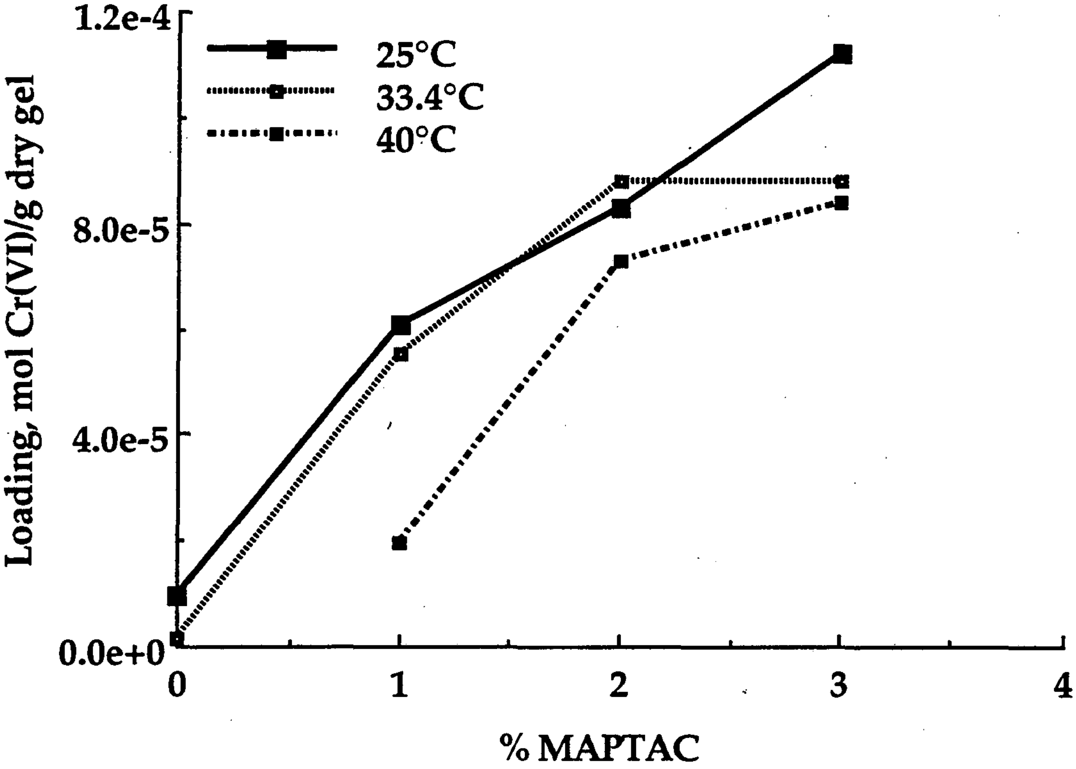

1.2e-4
8.0e-5
4.0e-5
0.0e+0
Loading, mol Cr(VI)/g dry gel
25°C
33.4°C
40°C
0
1
2
3
4
% MAPTAC

Figure 6

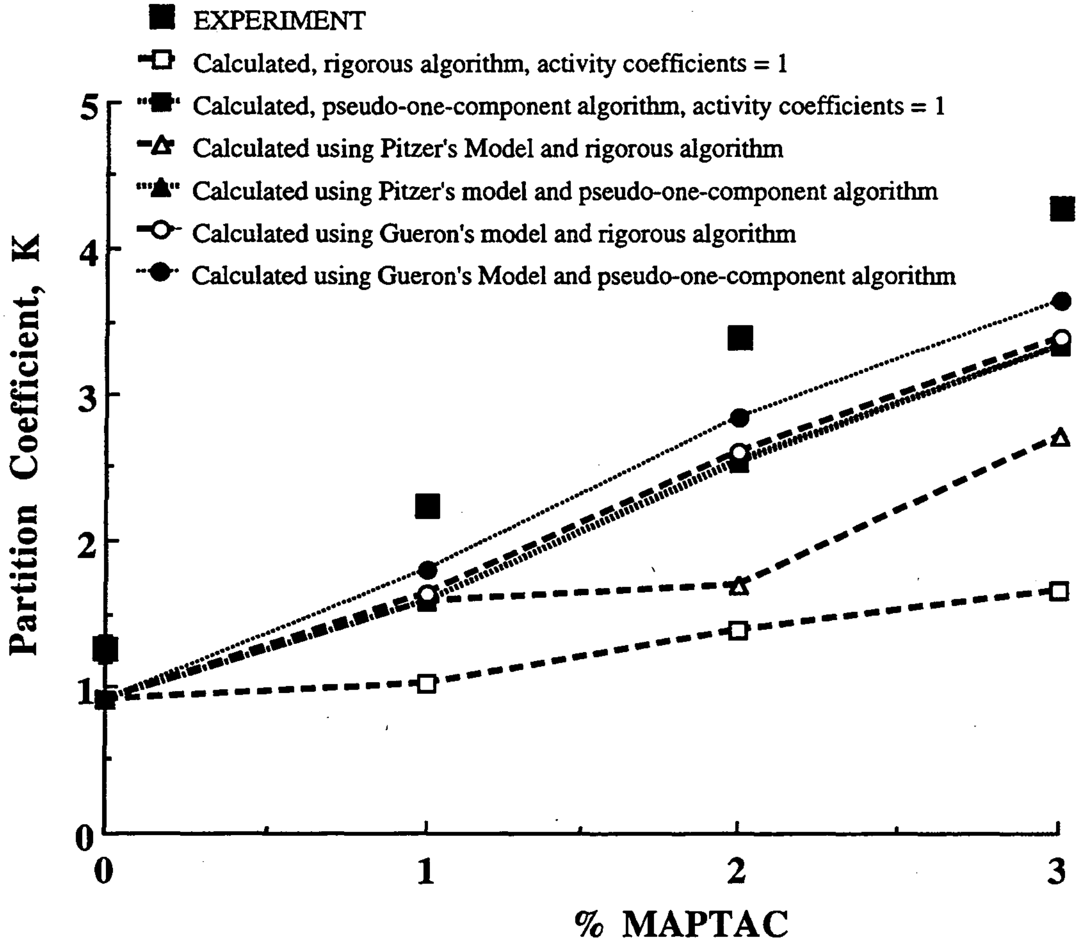
EXPERIMENT
Calculated, rigorous algorithm, activity coefficients = 1
Calculated, pseudo-one-component algorithm, activity coefficients = 1
Calculated using Pitzer's Model and rigorous algorithm
Calculated using Pitzer's model and pseudo-one-component algorithm
Calculated using Gueron's model and rigorous algorithm
Calculated using Gueron's Model and pseudo-one-component algorithm
Partition Coefficient, K
0
1
2
3
4
5
0
1
2
3
% MAPTAC

Figure 7

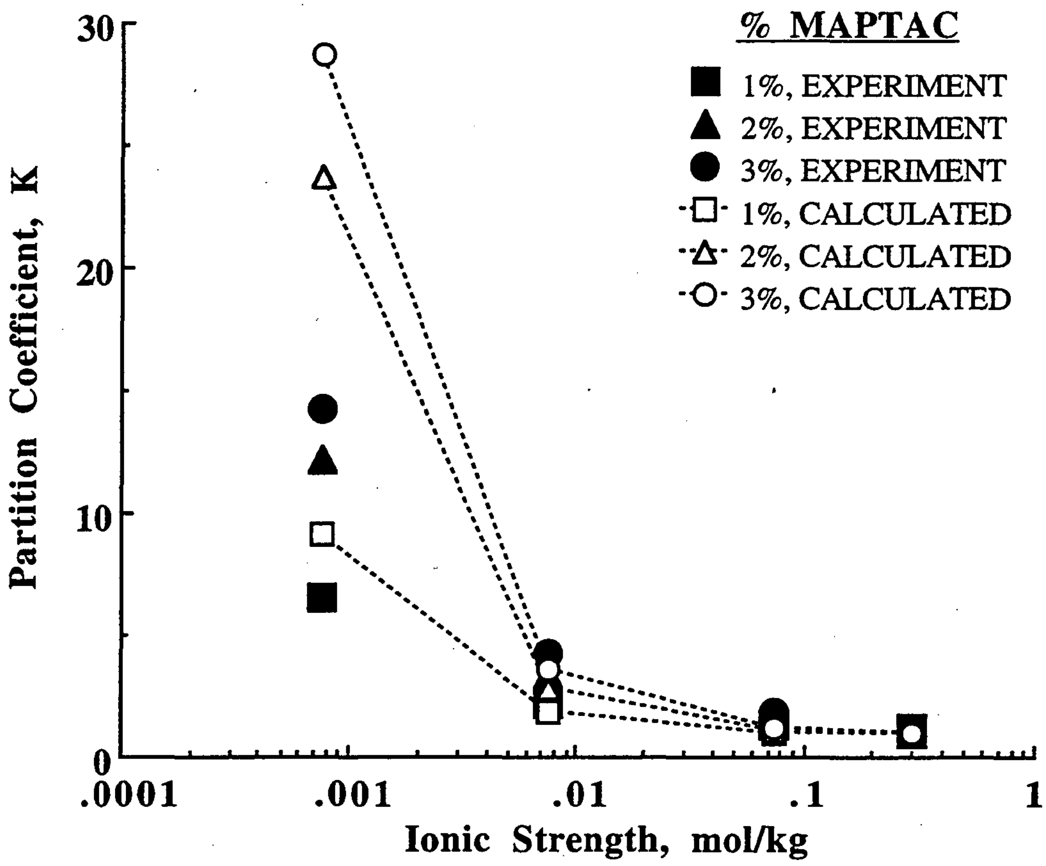
% MAPTAC
■ 1%, EXPERIMENT
▲ 2%, EXPERIMENT
● 3%, EXPERIMENT
-□- 1%, CALCULATED
-△- 2%, CALCULATED
-○- 3%, CALCULATED
Partition Coefficient, K
30
20
10
0
.0001
.001
.01
.1
1
Ionic Strength, mol/kg

Figure 8

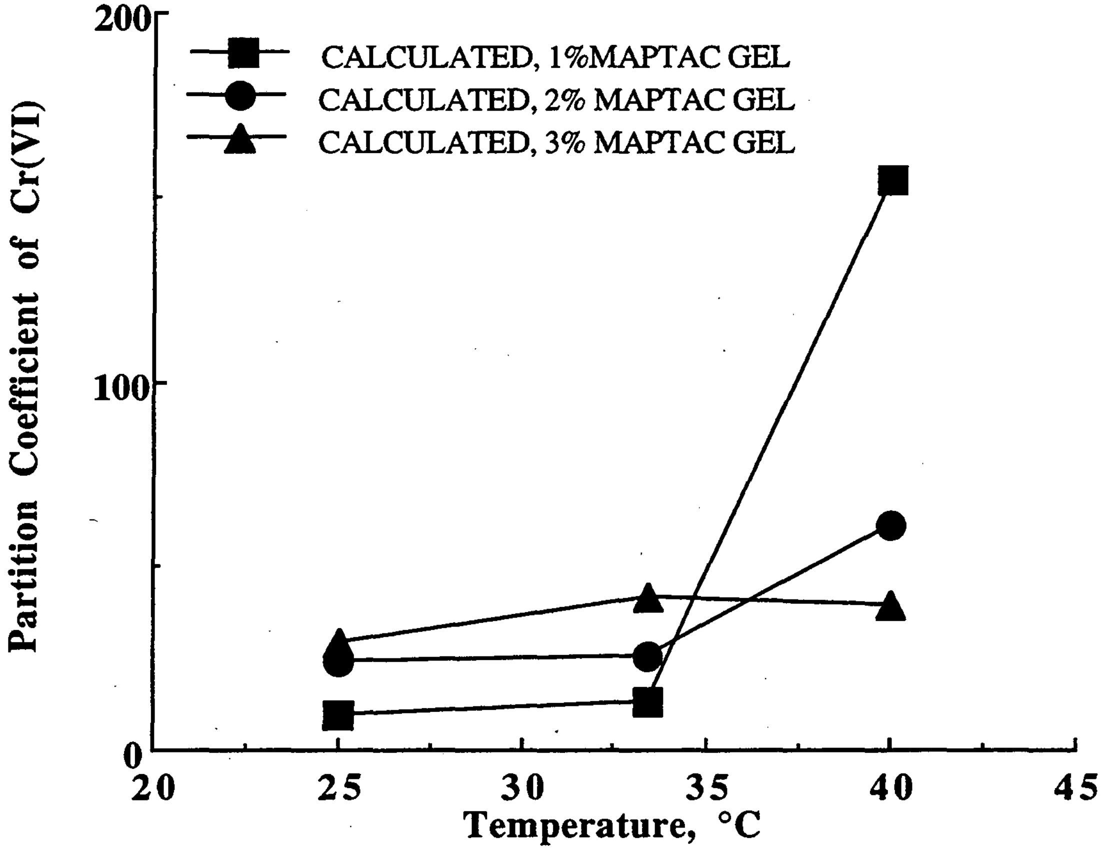

CALCULATED, 1%MAPTAC GEL
CALCULATED, 2% MAPTAC GEL
CALCULATED, 3% MAPTAC GEL
Partition Coefficient of Cr(VI)
200
100
0
20
25
30
35
40
45
Temperature, °C

TABLE 1

Ionic Strength-Dependent Swelling Equilibria in Aqueous Potassium Dichromate Solutions for poly-NIPA/MAPTAC Gels (15%T, 1%C)

	swelling ratio (g swollen gel/g dry gel) for specified %MAPTAC (%CM) at 10°C			
Ionic Strength mol/kg	0% MAPTAC	1% MAPTAC	2% MAPTAC	3% MAPTAC
1.0E-07	16.5 ± 0.2	34.3 ± 0.2	51. ± 1.	63.0 ± 0.4
3.0E-05	16.7 ± 0.2	23.1 ± 0.2	42.8 ± 0.5	55.5 ± 0.7
3.0E-04	16.17 ± 0.04	22.2 ± 0.3	36.9 ± 0.4	44.4 ± 0.2
3.0E-03	16.27 ± 0.05	18.4 ± 0.1	25.9 ± 0.8	29. ± 1.
3.0E-02	16.8 ± 0.1	18.1 ± 0.1	23.1 ± 0.5	23.6 ± 0.3
3.0E-01	17.5 ± 0.1	19.2 ± 0.4	24.8 ± 0.2	24.3 ± 0.3
4.5E-01	17.26 ± 0.06	19.2 ± 0.1	24.7 ± 0.1	24. ± 1.

TABLE 2

Effect of Ionic Strength on Partioning of Cr(VI) Between Aqueous Potassium Dichromate Solutions and poly-NIPA/MAPTAC Gels (15%T, 1%C, 0-3%CM)

Partition Coefficient, K, at 22°C

Ionic Strength	0% MAPTAC		1% MAPTAC		2% MAPTAC		3% MAPTAC	
mol/kg	experiment	calculated	experiment	calculated	experiment	calculated	experiment	calculated
7.5E-04	1.66 ± 0.02	0.91	6.53 ± 0.1	9.12	12.2 ± 0.2	23.65	14. ± 1.	28.71
7.5E-03	1.3 ± 0.1	0.91	2.23 ± 0.05	1.82	3.37 ± 0.05	2.84	4.27 ± 0.07	3.64
7.5E-02	0.92 ± 0.03	0.92	1.25 ± 0.06	1.02	1.85 ± 0.06	1.13	1.86 ± 0.08	1.22
3.0E-01	0.98 ± 0.09	0.91	1.21 ± 0.08	0.96	1.0 ± 0.2	0.98	1.124 ± 0.007	1.01

TABLE 3

Effect of Temperature on Partitioning of Cr(VI) Between Aqueous Potassium Dichromate Solutions and poly-NIPA/MAPTAC Gels (15%T, 1%C, 0-3%CM)

partition coefficient, K, from solutions of 0.00025 mol/kg potassium dichromate [26 mg/L]

Temperature	0% MAPTAC		1% MAPTAC		2% MAPTAC		3% MAPTAC	
°C	experiment	calculated	experiment	calculated	experiment	calculated	experiment	calculated
25	1.66 ± 0.02	0.91	6.5 ± 0.1	9.12	12.2 ± 0.2	23.65	14. ± 1.	28.78
33.4	0.42 ± 0.01	0.85	8.5 ± 0.3	12.74	13.7 ± 0.3	25.06	15.50 ± 0.05	41.40
40			38.6 ± 0.2	154.41	27. ± 3.	60.33	13.8 ± 0.9	38.89

TABLE 4

Comparison of Approaches to Calculating Partitioning of Cr(VI)Ions Between Aqueous Potassium Dichromate Solutions and poly-NIPA/MAPTAC Gels (15%T, 1%C, 0-3%CM)

partition coefficient, K, from a solution of 0.0025 mol/kg potassium dichromate at 22°C

		Rigorous Algorithm			Semi-Rigorous Algorithm		
%MAPTAC	experiment	Ideal*	Pitzer**	Guerón***	Ideal*	Pitzer**	Guerón***
0	1.26 ± 0.1	0.91	0.91	0.91	0.91	0.91	0.91
1	2.23 ± 0.05	1.01	1.58	1.63	1.58	1.58	1.81
2	3.37 ± 0.05	1.38	1.68	2.60	2.53	2.54	2.84
3	4.27 ± 0.07	1.66	2.70	3.39	3.32	3.33	3.64

*Ideal: All ionic activity coefficients are unity.

**Pitzer: Ionic activity coefficients calculated using the method of Pitzer, neglecting specific ion-ion interactions.

***Guerón: Ionic activity coefficients calculated using the method of Guerón and Weisbuch.

APPENDIX A

Calculating Partitioning of Cr(VI) Using the Rigorous Algorithm

In the rigorous algorithm, we explicitly consider the concentrations of all the mobile ions in the system. For the case under consideration, we have six ions: $Cr_2O_7^{2-}$, $HCrO_4^-$, CrO_4^{2-}, K^+, H^+, and OH^-. We also consider three chemical equilibria for these ions (17, 21):

$$HCrO_4^- \leftrightarrow H^+ + CrO_4^{2-}\text{, pK} = 6.5$$

$$2HCrO_4^- \leftrightarrow Cr_2O_7^{2-} + H_2O\text{, pK} = 1.52$$

$$H_2O \leftrightarrow H^+ + OH^-\text{, pK} = 14$$

We determine experimentally the total molarity of the chromate anions by measuring the absorbance of the bath solution in equilibrium with the gel, and we know that the solutions were originally prepared by dissolving potassium dichromate ($K_2Cr_2O_7$). We first calculate the ionic concentrations in the bath solution. To do so, we require six equations, as we have six unknowns. Three are provided by the chemical equilibria listed above. Two are provided by elemental balances on potassium and on chromate. The remaining equation is obtained by forcing the solution to be electroneutral. These six equations must be solved simultaneously to obtain the desired ion concentrations. Activity coefficients are included in calculations of chemical equilibria.

To obtain the six ion concentrations in the gel phase, we use the method outlined by Newman (35, 38). We characterize the bath solution containing the six ions by a set of independent, neutral components. For example, the set of two components could be $K_2Cr_2O_7$ and H_2O or $KHCrO_4$ and H_2O. Only two components are sufficient to characterize the solution completely because we know the equilibrium constants for the reactions between the ions. Because the solution was made by adding $K_2Cr_2O_7$ to H_2O, we used this set of independent, neutral components. We applied equation 2 (as developed in equations 8 and 9) to both components, giving two equations. The three chemical equilibria gave three more equations, and we obtained the sixth equation from the condition that the gel phase is electroneutral. The charge on the polymer backbone thus entered the calculation through the condition of electroneutrality. These six equations were then solved simultaneously for the six ion concentrations in the gel.

Our system is overspecified; we could have replaced the two chromate anion equilbria relations with equation 2 applied to $KHCrO_4$ and K_2CrO_4 (which are not independent components). Doing so, however, resulted in a set of six equations which were more difficult to solve, yielding ion concentrations which were slightly inconsistent with the known equilibria between the ions.

APPENDIX B

Calculating Partition Coefficients Using the Pseudo-One-Component Algorithm

We call this method of calculating the Cr(VI) partition coefficient the pseudo-one-component algorithm because, in applying it, we transform the weak electrolyte system of six ions characterized by two neutral components to a strong electrolyte system characterized by a single neutral component, a 1-1 salt.

We begin in the same manner as in the rigorous algorithm and calculate the concentrations of all the ions in the bath solution. From these concentrations, the ionic strength of the bath solution is known. At this point, we transform the model system (which corresponds to experiment) to a hypothetical system containing water, gel and a 1-1 salt (NaCl). In the hypothetical system, the concentration of the 1-1 salt in the bath solution is taken to be the ionic strength of the bath solution containing the six ions and water. In other words, the salt concentration of the bath solution of the system for which we are going to perform calculations is the same as the ionic strength of the bath solution in the experiment.

Our hypothetical system has only one component and thus two ions. We solve for the concentration of each ion in the gel phase by solving equation 2 constrained by an equation of electroneutrality of the gel phase. As before, the charges on the polymer are included in the condition of electroneutrality, and the counterions of the polyelectrolyte are taken to be one of the ions of the salt. The partition coefficient thus obtained for the anion is taken to be the partition coefficient of Cr(VI) because chromium is present only in the anions and because the univalent chromium anion ($HCrO_4^-$) contains only one chromium atom. We found that this procedure resulted in the best agreement between calculated and experimental partition coefficients. It is also much easier to solve two simultaneous equations as opposed to six.

APPENDIX C

Activity Coefficients in Solutions of Charged Hard-Spheres

1.Debye-Hückel Model

The Debye-Hückel (DH) activity coefficients are widely used due to their relatively simple analytical form. In the DH approach, the linearized Poisson-Boltzmann equation is solved for the potential and charge density as a function of radial distance from a central spherical ion in a solution of other spherical ions of the same diameter (25). Because the linear Poisson-Boltzmann equation is solved in DH, the DH activity coefficients agree well with experimental data only at low ionic strength, where the electrostatic potentials are low. Because DH activity coefficients are familiar, we present only the expression for the single-ion activity coefficient, γ_j. The reader is referred to reference (25) for a discussion regarding how γ_j is obtained from the solution to the Poisson-Boltzmann equation. Single ion activity coefficients (γ_j) in the Debye-Hückel theory are evaluated by:

$$\ln\gamma_j = -\frac{z_j^2 e^2 \kappa}{8\pi\varepsilon_0\varepsilon_r k_b T(1+\kappa a)} \tag{C.1}$$

where

$$\kappa^2 = \frac{e^2}{\varepsilon_o\varepsilon_r k_b T}\sum_k \rho_k z_k^2 \tag{C.2}$$

(κ is known as the inverse Debye screening length), e is the electronic charge, k_b is Boltzmann's constant, T is the temperature, ε_o is the vacuum permittivity, ε_r is the relative permittivity of the solvent (taken to be 78.5 for water), z_k is the valence of ionic species k, ρ_k is the number density (N_k/V) of species k, and a is the common diameter of all the ions. The sum extends over all ionic species.

2. Pitzer's Model

In Pitzer's expressions for the activity coefficient, electrostatic and specific non-electrostatic ion-ion interactions are taken into account (29). The leading term in Pitzer's expression represents the electrostatic contribution to the activity coefficient and is basically a semi-empirical modification of the Debye-Hückel expression for the electrostatic contribution. The remaining terms account for two-ion and three-ion specific interactions and are related to second and third osmotic virial coefficients. Pitzer's model is also widely used, and the ion-ion interaction parameters are available for many different salts, including chromates (29, 39). The general expression for the activity coefficient of a salt $M_{\nu_M}X_{\nu_X}$ in a multicomponent electrolyte solution is obtained by taking the partial derivative of Pitzer's expression for the excess Gibbs energy:

$$\begin{aligned}\ln\gamma_{MX} = {} & |z_M z_X|F + (\nu_M/\nu)\sum_a m_a[2B_{Ma} + ZC_{Ma} + 2(\nu_X/\nu_M)\Phi_{Xa}] \\ & + (\nu_M/\nu)\sum_c m_c[2B_{Mc} + ZC_{Mc} + 2(\nu_M/\nu_X)\Phi_{Xc}] \\ & + \sum_c \sum_a m_c m_a \nu^{-1}[2\nu_M z_M C_{ca} + \nu_M\psi_{Mca} + \nu_X\psi_{caX}] \\ & + \sum \sum_{c<c'} m_c m_{c'}(\nu_X/\nu)\psi_{cc'X} + \sum \sum_{a<a'} m_a m_{a'}(\nu_M/\nu)\psi_{aa'X} \\ & + 2\sum_n m_n(\nu_M\lambda_{nM} + \nu_X\lambda_{nX})/\nu \end{aligned} \qquad (C.3)$$

where the subscript a denotes anions, c denotes cations, n denotes neutral molecules, z_M and z_X are the valencies of the cation and anion, respectively, ν_M and ν_X are the stoichiometric coefficients of the cation and anion in the salt $M_{\nu_M}X_{\nu_X}$, $\nu = \nu_M + \nu_X$, $\Phi_{ii'}$ is a difference combination of the binary interaction parameters $\lambda_{ii'}$, and $\psi_{ii'j}$ is a difference combination of ternary interaction parameters. The parameters $\Phi_{ii'}$ and $\psi_{ii'j}$ are here set to zero. The remaining parameters are defined as follows:

$$F = f^{\gamma} + \sum_{c} \sum_{a} m_c m_a B'_{ca} + \sum \sum_{c<c'} m_c m_{c'} \Phi'_{cc'} + \sum \sum_{a<a'} m_a m_{a'} \Phi'_{aa'} \tag{C.4}$$

$$f^{\gamma} = -(4IA_{\phi}/b)\ln(1 + bI^{1/2}) \tag{C.5}$$

$$I = 0.5 \sum_{i \neq 0} m_i z_i^2 \tag{C.6}$$

$$A_{\phi} = (1/3)(2\pi N_{Av}\rho/1000)^{1/2}(e^2/4\pi\varepsilon_o\varepsilon_r k_b T)^{3/2} \tag{C.7}$$

$$B'_{MX} = [\beta^{(1)}_{MX} g'(\alpha_1 I^{1/2}) + \beta^{(2)}_{MX} g'(\alpha_2 I^{1/2})]/I \tag{C.8}$$

$$g'(x) = -2[1 - (1 + x + x^2/2)\exp(-x)]/x^2 \tag{C.9}$$

$$B_{MX} = \beta^{(0)}_{MX} + \beta^{(1)}_{MX} g(\alpha_1 I^{1/2}) + \beta^{(2)}_{MX} g(\alpha_2 I^{1/2}) \tag{C.10}$$

$$g(x) = 2[1 - (1 + x)\exp(-x)]/x^2 \tag{C.11}$$

$$Z = \sum_{i \neq 0} m_i |z_i| \tag{C.12}$$

$$C_{MX} = C^{\phi}/2|z_M z_X|^{1/2} \tag{C.13}$$

Here, subscript i denotes any species in solution except water (species 0). In equation C.4, the parameters Φ' are ionic-strength derivatives of the parameter Φ appearing in equation C.3; like Φ, these are set to zero. In equation C.7, written for SI units, N_{AV} is Avogadro's number, ρ is the solution density, e the electronic charge, ε_0 the permittivity of free space, ε_r the relative permittivity of the solvent, k_b the Boltzmann constant, and T is the temperature. In equations C.8 and C.10, the terms leading in $\beta^{(2)}_{MX}$ can be neglected for 1-1 and 1-2 salts. The parameter b is a universal parameter equal to 1.2 (kg/mol)$^{1/2}$, and α_1 is 2.0 (kg/mol)$^{1/2}$. The Pitzer binary ion-ion interaction parameters $\beta^{(0)}_{MX}$ and $\beta^{(1)}_{MX}$ and the ternary interaction parameter C^{ϕ}_{MX} for aqueous potassium chromates were taken from the compilation of Pitzer parameters published by Kim and Frederick (39).

In calculations using the Pitzer model where all the different ionic species were considered, the λ_{nM} and λ_{nX} parameters (ion-polymer interactions) were set to zero, because they are not independently available. Partition coefficients were also calculated with all B_{MX}, B'_{MX}, and C_{MX} parameters set to zero (no ion-ion virial terms); these partition coefficients were virtually identical to those calculated with the full model. The calculated partition coefficients show fair agreement with experimental data; however, the calculated coefficients are always less than the experimental ones which might imply the presence of favorable ion-polymer interactions. To investigate this possibility, we re-calculated partition coefficients using a salt-polymer interaction coefficient regressed from experimental data for salt partitioning into poly-NIPA gels (0%CM). As a simplification, we combined the two parameters λ_{nX} and λ_{nM} in the following manner:

$$\nu\bar{\lambda}_{MX} = \nu_M\lambda_{nM} + \nu_X\lambda_{nX} \tag{C.14}$$

so as to regress only one parameter. We expect that $\bar{\lambda}_{MX}$ might be a linear function with Cr(VI) molality; however, the dependence of $\bar{\lambda}_{MX}$ on Cr(VI) molality was found empirically to be semi-logarithmic. Due to the unexpected dependence of $\bar{\lambda}_{MX}$ on molality, we hesitate to attach a physical significance to $\bar{\lambda}_{MX}$.

Figure C.1 compares experimental and calculated partition coefficients for Cr(VI) in 0-3% CM NIPA/MAPTAC gels where the initial molality of $K_2Cr_2O_7$ was 0.0025 mol/kg and $\bar{\lambda}_{MX}$ = -0.233 kg/mol. Also shown are the partition coefficients calculated with $\bar{\lambda}_{MX} = 0$ (from Figure 6). Agreement between experimental and calculated coefficients improves significantly with the inclusion of the regressed value for $\bar{\lambda}_{MX}$, yet perfect agreement is still not obtained. Differences between nominal and actual %CM would not yield better agreement in this case, because the actual %CM would tend to be slightly less than the nominal value as suggested by atomic analysis for nitrogen composition of gels dried to constant weight.

We also calculated partition coefficients corresponding to the data at 33.4°C and found similar agreement. Our routine was unable to predict partition coefficients at 40°C and higher temperatures. At these temperatures, because the gel was sufficiently collapsed to raise the charge density, the routine did not converge.

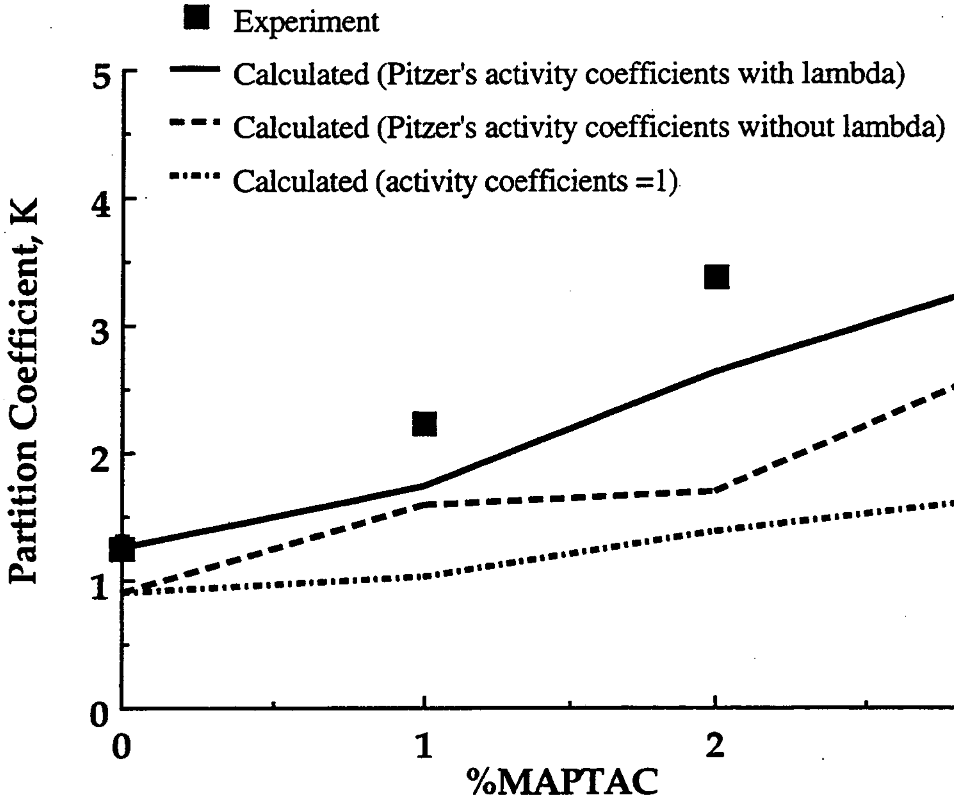

Figure C.1. Experimental (points) and calculated (lines) partition coefficients for Cr(VI) partitioning into 0-3%CM poly-NIPA/MAPTAC gels from a solution of initial molality of 0.0025 mol/kg potassium dichromate at 22°C. The dash-dot line denotes calculations where all activity coefficients were taken to be unity. The dashed line denotes calculations where Pitzer's activity coefficients were used, with all ion-ion specific interactions neglected. The solid line denotes calculations using Pitzer's activity coefficients with the inclusion of an ion-polymer interaction term, $\overline{\lambda}_{MX}$. Calculations were performed for 0, 1, 2, and 3% MAPTAC; the lines connect the results for these %CM. The rigorous algorithm was used in all cases.

3. The Mean Spherical Approximation

The Mean Spherical Approximation (MSA) is the result of using an integral equation for the description of ion-ion interactions in the primitive model of electrolyte solutions (26, 40, 41). Unlike Debye-Hückel-type theories, all of the ions need not have the same diameter in the MSA. The MSA has been shown to give good results for activity coefficients up to moderate ion concentrations (35). A major advantage of the MSA over other integral-equation theories is that its solution is analytical, and, therefore, the MSA is more amenable to use in phase equilibrium calculations than theories which must be evaluated numerically.

To find the excess thermodynamic properties of an ion in the MSA, one must solve a complicated implicit algebraic equation for the screening factor, Γ. While the equation is not difficult to solve for the screening factor, the expressions for partial thermodynamic properties, such as the chemical potential and activity coefficient, become extremely complicated and difficult to solve because one must differentiate the screening factor. Several explicit approximations to the MSA have been developed in an attempt to circumvent the solving implicitly for Γ. Harvey et al have investigated the deviation between the exact MSA and two explicit approximations in the calculation of various thermodynamic properties, including the chemical potential of an ion (27). The simplest explicit approximation is to use a single effective diameter for all ions. In the single-effective-ion-diameter (SID) approximation to the MSA, the single-ion activity coefficient for an ion j due to ion-ion coulombic interactions between charged hard spheres is given by:

$$\ln(\gamma_j) = -\frac{\Gamma^3}{\pi}\left[\frac{(1+\sigma_{mix}\Gamma)z_j^2}{\sum\limits_k \rho_k z_k^2} - \frac{\Gamma}{\rho}(\sigma_j - \sigma_{mix})\right] \tag{C.15}$$

where

$$\rho\sigma_{\mathrm{mix}} = \sum_{k} \rho_k \sigma_k \tag{C.16}$$

$$\rho = \sum_{k} \rho_k \tag{C.17}$$

$$\Gamma = \frac{1}{2\sigma_{\mathrm{mix}}}\left[\left(1 + 2\sigma_{\mathrm{mix}}\kappa\right)^{1/2} - 1\right] \tag{C.18}$$

$$\kappa^2 = \frac{e^2}{\varepsilon_o \varepsilon_r k_b T} \sum_{k} \rho_k z_k^2 \tag{C.19}$$

(κ is the reciprocal Debye screening length), *e* is the electronic charge, k_b is Boltzmann's constant, T is the temperature, ε_o is the vacuum permittivity, ε_r is the relative permittivity of the solvent (taken to be 78.5 for water), z_k is the valence and σ_k the diameter of species k, and ρ_k is the number density (N_k/V) of species k. The sums extend over all ionic species. The MSA screening parameter, Γ, is similar to the reciprocal Debye screening length, κ; Γ tends to $\kappa/2$ at infinite dilution.

Excess Chemical Potential in the Exact MSA

To illustrate the considerable simplification introduced by using the SID approximation, the exact MSA expression for the excess chemical potential is presented below:

$$k_b T \ln\left(\gamma_j\right) = \frac{\partial\left(A^{ex}/V\right)}{\partial \rho_j} \tag{C.20}$$

$$\frac{A^{ex}}{V} = -\frac{e^2}{4\pi\varepsilon_o\varepsilon_r}\left(\Gamma \sum_{k} \frac{\rho_k z_k^2}{1 + \sigma_k \Gamma} + \frac{\pi}{2\Delta}\Omega P_n^2\right) + \frac{\Gamma^3 kT}{3\pi} \tag{C.21}$$

$$\Delta = 1 - \frac{\pi}{6}\sum_{k} \rho_k \sigma_k^3 \tag{C.22}$$

$$\Omega = 1 + \frac{\pi}{2\Delta}\sum_k \frac{\rho_k \sigma_k^3}{1+\sigma_k \Gamma} \tag{C.23}$$

$$P_n = \frac{1}{\Omega}\sum_k \frac{\sigma_k \rho_k z_k}{1+\sigma_k \Gamma} \tag{C.24}$$

$$4\Gamma^2 = \frac{\kappa^2 \sum_k \rho_k (1+\sigma_k \Gamma)^{-2} (z_k - \pi \sigma_k P_n/2)^2}{\sum_k \rho_k z_k^2} \tag{C.25}$$

APPENDIX D

Activity Coefficients from the Cell Model

Guerón and Weisbuch have derived simple analytical expressions for the activity coefficients of univalent ions in a polyelectrolyte solution (34). These expressions are not exact, in that they are not obtained by taking partial derivatives of the electrostatic energy, which, for a solution containing polyelectrolyte and added salt, must be obtained numerically. They are instead derived from general properties of numerical solutions to the Poisson-Boltzmann equation. The reader is referred to reference (34) for details on the derivation of these activity coefficients. We also discuss the cell model in reference 30.

For a univalent counterion, the activity coefficient is given by the following expression:

$$\gamma_{\text{counterion}} = \frac{0.7\aleph/\xi + 1}{\aleph + 1} \tag{D.1}$$

For a univalent coion, the activity coefficient is given by the following expression:

$$\gamma_{\text{coion}} = \frac{0.7\aleph/\xi + 1}{0.53\aleph/\xi + 1} \tag{D.2}$$

where $\aleph$ is the ratio of concentration of charged monomers (u in the standard notation of the cell model) to salt concentration (n in the standard notation of the cell model), and ξ is the polyelectrolyte linear charge density defined by the ratio of the Bjerrum length, $\Im$, to the monomer length, b:

$$\xi = \frac{\Im}{b} = \frac{e^2}{4\pi\varepsilon_o\varepsilon_r k_b T b} \tag{D.3}$$

The Bjerrum length is the distance between univalent ions in a dielectric medium where the coulombic energy is equal to k_bT; approximately 7.14 Å in pure water at room temperature.

For an ion of valence z, Guerón and Weisbuch propose to substitute $|z|\xi$ for ξ in the above equations for the activity coefficient of the counterion and the coion to a polyelectrolyte (34). That the activity coefficients for a multivalent ion should be such a simple transformation from the activity coefficients for a univalent ion is questionable, because we see no reason why the effect of the increase in valency from unity to z of an ion can be "transferred" to the charged cylinder simply by increasing its linear charge density from ξ to $|z|\xi$ (42).

We wish to emphasize several remarks made by Guerón and Weisbuch regarding these simple expressions. First, their expressions are only approximations to the activity coefficients of ions in the cell model (which by nature, neglects ion-ion electrostatic interactions) and should be most accurate when $\aleph$ is low, for example, less than 1. We calculated partition coefficients using these activity coefficients and compared the coefficients to those calculated with numerical solutions available in the literature (43, 44). The coefficients calculated using the activity coefficient expressions of Guerón and Weisbuch reproduced the coefficients calculated using the numerical solutions to the Poisson-Boltzmann equation best at low $\aleph$, but surprisingly agreed better with the experimental data for partitioning of Cr(VI) even when $\aleph$ was greater than unity. We therefore used Guerón and Weisbuch's activity coefficients for all calculations of Cr(VI) partitioning in our highly swollen hydrogels. Second, the activity coefficient for the co-ion is greater than unity, unlike the Debye-Hückel and MSA activity coefficients, which do not exceed unity. Third, the dependence of the activity coefficient on valence of an ion, as proposed by Guerón and Weisbuch, is much different qualitatively from those in Debye-Hückel, MSA or Pitzer's models. We emphasize that it is meaningless to compare numerical activity coefficients obtained from the cell model to those obtained from a charged-hard-sphere theory because the activity coefficients are measures of different electrostatic effects in the two types of theories.

NOMENCLATURE

Roman

a_j	diameter of ion j (m)
a_i	activity of component i
A	Helmholtz energy (J)
A^{ex}	excess Helmholtz energy (J)
A^{ideal}	ideal Helmholtz energy (J)
A_ϕ	Debye-Hückel coefficient for the osmotic coefficient (kg mol^{-1}) (defined in Appendix C)
Å	angstrom (10^{-10} m)
b	parameter in expression for single-ion activity coefficients of Pitzer (kg$^{0.5}$ mol$^{-0.5}$)
b	monomer length (m)
B_{MX}	combination of parameters in Pitzer's expression for single-ion activity coefficients (defined in Appendix C)
B'_{MX}	combination of parameters in Pitzer's expression for single-ion activity coefficients (defined in Appendix C)
C_{MX}	combination of parameters in Pitzer's expression for single-ion activity coefficients (defined in Appendix C)
C^{ϕ}_{MX}	ternary interaction parameter in Pitzer's expression for single-ion activity coefficients
%C	percent crosslinking monomer
%CM	percent comonomer
e	electronic charge (1.6022×10^{-19} C)
F	combination of parameters in Pitzer's expression for single-ion activity coefficients (defined in Appendix C)

f^{γ}	combination of parameters in Pitzer's expression for single-ion activity coefficients (defined in Appendix C)
$g(x)$	function in Pitzer's expression for single-ion activity coefficients (defined in Appendix C)
$g'(x)$	function in Pitzer's expression for single-ion activity coefficients (defined in Appendix C)
H	hydration
I	ionic strength (mol kg^{-1})
K	partition coefficient
k_b	Boltzmann's constant (1.381×10^{-23} J K^{-1})
m_i	measure of concentration of component i (mol m^{-3})
n_i	mole number of component i (mol)
N_{AV}	Avogadro's number (6.02×10^{23} mol^{-1})
N_j	number of species j
P^{ex}	excess pressure (Pa)
pH	negative the base ten logarithm of the activity of the hydrogen ion
pK	negative the base ten logarithm of the equilibrium dissociation constant
P_n	parameter in the MSA (defined in Appendix C)
R	universal gas constant (8.314 J mol^{-1} K^{-1})
T	temperature (K)
%T	ratio of monomer to diluent at synthesis (g mL^{-1})
V	volume (m^3)
$\overline{V}_i$	partial molar volume of component i (m^3 mol^{-1})
z_j	valence of species j
Z	combination of parameters in Pitzer's expression for single-ion activity coefficients (defined in Appendix C)

Greek, Hebrew, and Symbols

$\aleph$	ratio of concentration of charged monomers to concentration of monovalent salt
$\Im$	Bjerrum length (m)
α_1	parameter in Pitzer's expression for single-ion activity coefficients ($kg^{0.5}$ $mol^{-0.5}$)
$\beta_{MX}^{(0)}$	binary interaction parameter in Pitzer's expression for single-ion activity coefficients
$\beta_{MX}^{(1)}$	binary interaction parameter in Pitzer's expression for single-ion activity coefficients
$\beta_{MX}^{(2)}$	binary interaction parameter in Pitzer's expression for single-ion activity coefficients
Δ	combination of parameters in the MSA (defined in Appendix C)
ε_o	vacuum permittivity (C^2 J^{-1} m^{-1})
ε_r	relative permittivity
$\Phi_{ii'}$	combination of parameters $\lambda_{ii'}$ in Pitzer's expression for single-ion activity coefficients (set to zero in this work)
$\Phi'_{ii'}$	combination of parameters in Pitzer's expression for single-ion activity coefficients (defined in Appendix C)
γ_i	activity coefficient of component i
γ_j	single-ion activity coefficient of ionic species j
γ_+	single-ion activity coefficient for a cation
γ_-	single-ion activity coefficient for an anion
$\gamma_\pm$	mean ionic activity coefficient for a salt
Γ	screening parameter in the Mean Spherical Approximation (m^{-1})
κ	inverse Debye screening length (m^{-1})

$\lambda_{ii'}$	binary interaction parameter between species i and i' in Pitzer's expression for single-ion activity coefficients (kg mol^{-1})
$\overline{\lambda}_{MX}$	mean salt-polymer interaction parameter (kg mol^{-1})
μ_i	chemical potential of component i (J mol^{-1})
μ_i^o	standard state chemical potential of component i (J mol^{-1})
ν_j	stoichiometric coefficient of ion j
ν	sum of stoichiometric coefficients of ions which constitute a neutral salt
$\Delta\Pi_{elastic}$	elastic contribution to swelling pressure (Pa)
ρ_j	number density of ion j (m^{-3})
ρ	total number density of solution ($\sum_j \rho_j$) (m^{-3})
σ_j	diameter of ion j (m)
σ_{mix}	average diameter of all ions in solution (defined in Appendix C) (m)
Ω	parameter in the MSA (defined in Appendix C)
ξ	dimensionless linear charge density
$\psi_{ii'}$	combination of ternary interaction parameters in Pitzer's expression for single-ion activity coefficients (set to zero in this work)

REFERENCES

1. J. H. Priest, S. L. Murray, R. J. Nelson, and A. S. Hoffman, *Lower Critical Solution Temperatures of Aqueous Copolymers of N-isopropylacrylamide and Other N-substituted Acrylamides* in Reversible Polymeric Gels and Related Systems, Paul Russo, ed. (American Chemical Society, Washington D.C., 1987).
2. S. Beltrán, H. H. Hooper, H. W. Blanch, and J. M. Prausnitz, Journal of Chemical Physics **92**, 2061 (1990).
3. S. Beltrán, J. P. Baker, H. H. Hooper, H. W. Blanch, and J. M. Prausnitz, Macromolecules **24**, 549 (1990).
4. S. J. Trank, D. W. Johnson, and E. L. Cussler, Food Technology **43**, 76 (1989).
5. D. C. Roepke, S. M. Goyal, C. J. Kelleher, D. A. Halvorson, A. J. Abraham, R. F. S. Freitas, and E. L. Cussler, Journal of Virological Methods **15**, 25 (1987).
6. Y. Hirokawa and T. Tanaka, Journal of Chemical Physics **81**, 6379 (1984).
7. M. Heskins and J. E. Guillet, J. Macromol. Sci., Chem. **A2**, 1441 (1968).
8. L. C. Dong and A. S. Hoffman, Journal of Controlled Release **4**, 223 (1986).
9. T. Okano, Y. H. Bae, H. Jacobs, and S. W. Kim, Journal of Controlled Release **11**, 255 (1990).
10. A. P. Sassi, H. W. Blanch, and J. M. Prausnitz, *Crosslinked Gels As Water Absorbents in Separations* in Polymer Applications for Biotechnology, D. Soane, ed. (Englewood Cliffs: Prentice Hall, 1992)
11. E. L. Cussler, M. R. Stokar, and J. E. Vararbert, AIChE Journal **30**, 578 (1984).
12. S. Gehrke, *Synthesis, Equilibrium Swelling, Kinetics, Permeability, and Applications of Environmentally Responsive Gels* in Responsive Gels: Volume Transitions II, K. Dusek, ed.(Berlin: Springer-Verlag, 1993)
13. L. H. Lyu and S. H. Gehrke, *Final Project Report: Dewatering Fine Coal Slurries by Gel Extraction* Ohio Coal Development Office, Columbus, Ohio., 1990)

14. E. Vasheghani-Farahani, D. G. Cooper, J. Vera, and M. E. Weber, Chemical Engineering Science **47**, 31 (1992).

15. A. K. Sengupta and D. Clifford, Industrial Engineering and Chemistry Fundamentals **1986**, 249 (1986).

16. A. K. Sengupta and D. Clifford, Reactive Polymers **4**, 113 (1986).

17. A. K. Sengupta, T. Roy, and D. Jessen, Reactive Polymers **9**, 293 (1988).

18. T. V. Arden and M. Giddings, J. Appl. Chem. **11**, 229 (1961).

19. M. W. Heininger and C. E. Meloan, Solvent Extraction and Ion Exchange **10**, 159 (1992).

20. M. Chanda and G. L. Rempel, Reactive Polymers **21**, 77 (1993).

21. J. Y. Tong and E. L. King, **75**, 6180 (1953).

22. G. P. Haight Jr., D. C. Richardson, and N. H. Coburn, Inorganic Chemistry **3**, 1777 (1964).

23. J. P. Baker, Equilibrium Swelling Properties of Ionized Hydrogels. Ph.D. thesis, University of California/Berkeley (1993).

24. L. Y. Chou, Buffer Effects on Aqueous Swelling Kinetics of Polyelectrolyte Gels. M.S. thesis, University of California/Berkeley (1991).

25. D. A. McQuarrie, *Statistical Mechanics* (Harper and Row, New York, 1975).

26. L. Blum and J. S. Høye, Journal of Physical Chemistry **81**, 1311 (1977).

27. A. H. Harvey, T. W. Copeman, and J. M. Prausnitz, Journal of Physical Chemistry **92**, 6432 (1988).

28. G. Mayorga and K. S. Pitzer, Journal of Physical Chemistry **77**, 2300 (1973).

29. K. S. Pitzer, *Activity Coefficients in Electrolyte Solutions* (Boca Raton: CRC Press, 1991)

30. A. P. Sassi, H.W. Blanch, and J.M. Prausnitz, *Phase Equilibria for Aqueous Protein/Polyelectrolyte Gel Systems*, LBL-36406, submitted to AIChE Journal, 1994.

31. S. Lifson and A. Katchalsky, Journal of Polymer Science **13**, 43 (1954).

32. A. Katchalsky, Z. Alexandrowicz , and O. Kedem, *Polyelectrolyte Solutions* in Chemical Physics of Ionic Solutions (Wiley, New York, 1966).

33. A. Katchalsky, Pure and Applied Chemistry **26**, 327 (1971).

34. M. Guerón and G. Weisbuch, J. Phys. Chem. **83**, 1991 (1979).

35. C. A. Haynes, Separation of Protein Mixtures by Extraction: Statistical-Mechanical Models of Aqueous Solutions Containing Polymers, Salts, and Globular Proteins. Ph.D. thesis, University of California/Berkeley (1992).

36. P. J. Flory, *Principles of Polymer Chemistry* (Cornell University Press, Ithaca, 1953).

37. H. M. James and E. Guth, Journal of Chemical Physics **15**, 669 (1947).

38. J. S. Newman, *Electrochemical Systems* (Prentice Hall, Englewood Cliffs, 1991).

39. H.-T. Kim and W. J. Frederick Jr., Journal of Chemical Engineering Data **33**, 177 (1988).

40. E. Waisman and J. L. Lebowitz, Journal of Chemical Physics **52**, 4307 (1970).

41. L. Blum, Molecular Physics **1975**, 1529 (1975).

42. D. Stigter, personal communication with the author, 1994.

43. D. Stigter, Journal of Colloid and Interfacial Science **53**, 296 (1975).

44. B. Kure Klein, C. F. Anderson, and M. T. Record, Biopolymers **20**, 2263 (1981).